MECHANISM AND KINETICS OF THE DEHYDRATION OF HYDRARGILLITES. PART I

F. PAULIK, J. PAULIK

Institute for General and Analytical Chemistry, Technical University of Budapest, Budapest (Hungary)

R. NAUMANN, K. KÖHNKE and D. PETZOLD

Chemistry Section, Mining Academy Freiberg, 9200 Freiberg (G.D.R.)

(Received 19 August 1982)

ABSTRACT

The decomposition mechanism of natural and artificial hydrargillites was investigated by means of quasi-isothermal–quasi-isobaric thermogravimetry and X-ray examination. It was shown that the decomposition of artificial hydrargillites consists of three partial reactions

$$\alpha\text{-Al(OH)}_3 \rightarrow \alpha\text{-AlOOH} + H_2O \tag{1}$$

$$2\,\alpha\text{-Al(OH)}_3 \rightleftarrows \chi\,Al_2O_3 + 3\,H_2O \tag{2}$$

$$2\,\alpha\text{-AlOOH} \rightleftarrows \gamma\text{-Al}_2O_3 + H_2O \tag{3}$$

Each of these partial reactions is divided into further partial processes, some of which take place in a quasi-isothermal, and some in a non-isothermal way, and part of them leads to equilibrium whereas the other part does not.

It was also shown that the decomposition of natural hydrargillites only takes place in the borderline case according to eqn. (2) and no boehmite is formed. However, between the two borderline cases the transition regarding the decomposition mechanism is continuous.

INTRODUCTION

There are numerous papers dealing with the examination of the thermal decomposition of hydrargillite which in the literature is also called gibbsite or, according to international nomenclature [1] $\alpha\text{-Al(OH)}_3$. The reason for such intensive investigation of this compound lies in the fact that thermal treatment of hydrargillite produces various modifications of aluminium oxide up to $\alpha\text{-Al}_2O_3$ and the transitional modifications of alumina, in particular, can find a versatile application in industry. Despite the application of various methods the results obtained are different and the dehydration processes supposed can actually be classified into four groups.

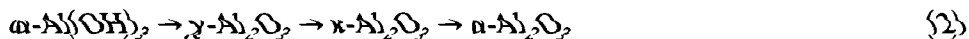*(1) The gradual decomposition of hydrargillite through boehmite*

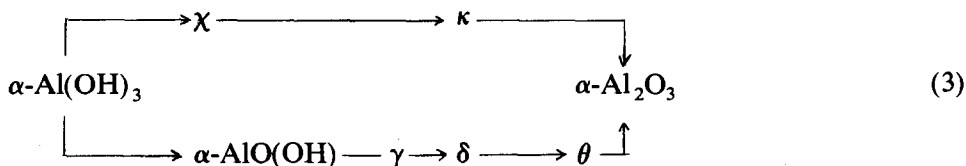According to Haber [2], Frary [3] and Zivkovic [4] the following process takes place

$$\alpha\text{-Al(OH)}_3 \rightarrow \alpha\text{-AlO(OH)} \rightarrow \gamma\text{-Al}_2\text{O}_3 \rightarrow \alpha\text{-Al}_2\text{O}_3 \qquad (1)$$
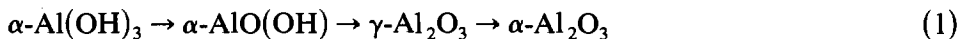
Stumpf et al. [5] observed before the appearance of the γ- form also χ-Al$_2$O$_3$ and thereafter κ- and θ-Al$_2$O$_3$. Tertian [6] obtained κ-Al$_2$O$_3$ instead of γ-Al$_2$O$_3$ and in the case of finely granulated samples the decomposition led directly to χ-Al$_2$O$_3$. Day and Hill [7,8] found also δ- and θ-Al$_2$O$_3$ between γ- and α-Al$_2$O$_3$. Sasvári and Hegedüs [9,10] reported on the existence of unstable boehmite formed from hydrargillite, in contrast with the stable boehmite formed from bayerite, and attributed the effects different from equation (1) to the bayerite content of the artificial hydrargillite. Beretka and Ridge [11] investigated the problem in vacuum and also observed the gradual decomposition according to eqn. (1).

(2) Decomposition of hydrargillite directly to χ-Al$_2$O$_3$

In the case of poorly crystallized samples, Goswami and Grupta [12] observed the reaction

$$\alpha\text{-Al(OH)}_3 \rightarrow \gamma\text{-Al}_2\text{O}_3 \rightarrow \kappa\text{-Al}_2\text{O}_3 \rightarrow \alpha\text{-Al}_2\text{O}_3 \qquad (2)$$

According to Day and Hill [7,8], χ-Al$_2$O$_3$ is always formed from hydrargillite which transforms through rehydration into boehmite. Ginsberg et al. [13] obtained this dehydration process with hydrargillite precipitated from potassium hydroxide solution. According to Sato et al. [14] the direct transformation takes place in finely pulverized hydrargillite.

(3) Two-branched reaction with primary formation of χ-Al$_2$O$_3$ and boehmite

$$
\begin{array}{l}
\quad\;\;\rightarrow \chi \longrightarrow \kappa \longrightarrow \\
\alpha\text{-Al(OH)}_3 \qquad\qquad\qquad \alpha\text{-Al}_2\text{O}_3 \qquad (3)\\
\quad\;\;\rightarrow \alpha\text{-AlO(OH)} - \gamma \rightarrow \delta \longrightarrow \theta
\end{array}
$$

This decomposition process was first observed by Brown et al. [15] and was the source of many new studies and interpretations. According to De Boer et al. [16], boehmite would be formed only under hydrothermal conditions. Tertian et al. [17] found that in vacuum mainly boehmite is formed. Saalfeld [18] confirmed the two-branched process also for the decomposition of hydrargillite monocrystals but did not find any δ-Al$_2$O$_3$. Kalinina [19], in contrast with most of the other authors, observed in the first step at 190°C

the formation of χ-Al_2O_3 and at 260°C a mixture of boehmite, χ- and γ-Al_2O_3. Already from 120°C upwards, Glemser and Rieck [20] obtained boehmite and ϵ-Al_2O_3. Ginsberg et al. [13] attribute the two-branched reaction to the presence of boehmite in the aluminium hydroxide obtained in the course of the Bayer process. Rouquerol et al. [21,22], in contrast with the findings of Beretka and Ridge [11], confirmed the performance of the two-branched reaction also in vacuum. Sato et al. [14] observed the partial boehmite formation only in the case of coarse crystalline hydrargillite. Many other researchers [23–31] also found that the decomposition of hydrargillite takes place according to the mechanism described above.

(4) Two-branched reaction with primary formation of $Al_2O_3 \cdot 2\ H_2O$ and boehmite

$$\begin{array}{c} \underset{}{\boxed{}} \xrightarrow{\quad} Al_2O_3 \cdot 2\ H_2O \xrightarrow{\quad} \chi \to \kappa \longrightarrow \\ \alpha\text{-}Al(OH)_3 \qquad\qquad\qquad\qquad \alpha\text{-}Al_2O_3 \qquad (4) \\ \longrightarrow \alpha\text{-}AlO(OH) \longrightarrow \chi \to \delta - \theta \longrightarrow \end{array}$$

By evaluating X-ray diagrams of various decomposition products of hydrargillites, Ashimesh Dutt and Bhaskar Rao [32] observed the presence of $Al_2O_3 \cdot 2\ H_2O$ before the formation of χ-Al_2O_3. As literature data prove, examination of the thermal decomposition of hydrargillite has led so far to many, often contradictory results.

We also studied the decomposition mechanism of hydrargillites [33–37]. From the obtained simultaneous TG and DTG curves of natural and artificial samples, similar to those illustrated in Figs. 1 and 2, the following conclusions could be drawn [33–35]. The decomposition can be in one stage (natural hydrargillite) or three stages (artificial hydrargillite) but between the

Fig. 1. TG (1–6) and Q-TG (7–12) curves of natural (I–III) and artificial (IV–VI) hydrargillites.

two borderline cases the transition is continuous. In the first and third periods of the decomposition the amount of the departing water changes proportionately, i.e., between the two processes there exists a causal relation.
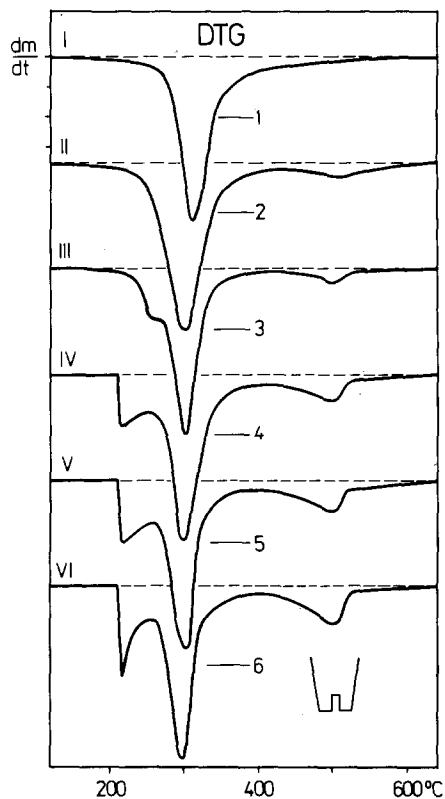

Fig. 2. DTG curves (1–6) of natural (I–III) and artificial (IV–VI) hydrargillites.

These regularities seemed to support the assumption of the two-branched decomposition mechanism [36].

Later, by investigating this problem with the method of quasi-isothermal–quasi-isobaric thermogravimetry [38,39], we also succeeded in detecting that the three-stage decomposition of hydrargillites is composed of several overlapping processes which are of different character [37]. Because of the great resolution and selectivity of this measuring technique, it was used to study this question further. The results of our examinations are summarized in the present work.

EXPERIMENTAL

Materials

The examinations were performed using six hydrargillite samples (I–VI) of different origin. Three of the samples (I, Szőc; II, Iszkaszentgyörgy; and

III, Határvölgy, Hungary) were of natural origin. These were probably formed upon hydrothermal effects in rock crevices by the side of bauxite deposit faults. X-Ray data of these samples (d-values measured in Å and the corresponding intensity values in parentheses) are:

sample I: 4.83(100);   4.36(30);   4.32(15);   2.38(14);   2.45(9)

sample II: 4.90(100);   4.38(40);   4.34(20);   2.39(14);   2.45(12)

Samples IV and V were the industrial products of Hungarian Alumina Factories from Magyaróvár and Almásfüzitő, respectively. Sample VI was also an industrial product of Alumina Factorie from Lauta (GDR).

The purity of sample VI was controlled and it was stated to contain 0.029% SiO_2, 0.028% Fe_2O_3 and 0.247% Na_2O. This sample, representing a borderline case, was investigated more thoroughly. Its grain size varied between 63 and 100 μm. X-Ray data (d-values measured in Å and the corresponding intensity values in parentheses) are: 4.86 (100); 4.37 (25); 4.31 (13); 2.38 (10); 2.45 (8). Literature [5] data are: 4.82 (100); 4.34 (40); 4.30 (13); 2.37 (20); 2.44 (15).

For calibration purposes in the X-ray investigation a boehmite was used which had been prepared from hydrargillite in an autoclave. This contained 0.071% SiO_2, 0.005% Fe_2O_3 and 0.263% Na_2O as impurities. X-Ray data (d-values, in Å and the corresponding intensities in parentheses) are: 6.12 (100); 3.16 (70); 2.34 (60); 1.86 (40); 1.85 (40). Literature [41] data are: 6.11 (100); 3.16 (65); 2.34 (53); 1.86 (32); 1.85 (27).

Thermoanalytical examinations

The conventional simultaneous TG and DTG examinations [39] and the quasi-isothermal–quasi-isobaric thermogravimetric measurements [38,39] were carried out using a Derivatograph-Q (Hungarian Optical Works MOM-Budapest).

Curves 1–6 in Figs. 1 and 2 were obtained for hydrargillite I–VI, at a heating rate of 5°C min^{-1}, in an open crucible, and in the presence of air. The weight of the samples amounted to about 300 mg.

For the sake of comparison, Fig. 1 shows both the conventional TG curves (curves 1–6) and the Q-TG curves (curves 7–12) of the same samples. The latter were obtained by applying the quasi-isothermal–quasi-isobaric measuring technique [37–39]. The 300 mg sample was placed in an open crucible and heated in the weight constant period at a heating rate of 3°C min^{-1}. The decomposition rate was controlled with 0.3 mg min^{-1} (calculated for 100 mg total weight change).

In the Q-TG curves isothermal and non-isothermal sections were observed. It was supposed that the isothermal decomposition processes lead to equilibrium, while the non-isothermal ones do not. Therefore, the borderline case representing two samples (I and VI) and a sample transitional type (III)
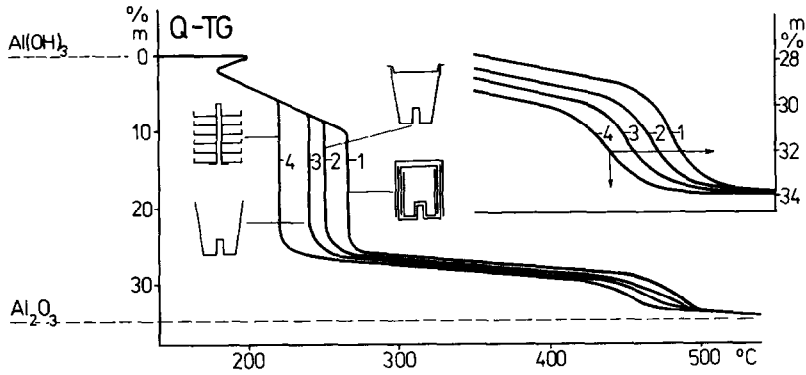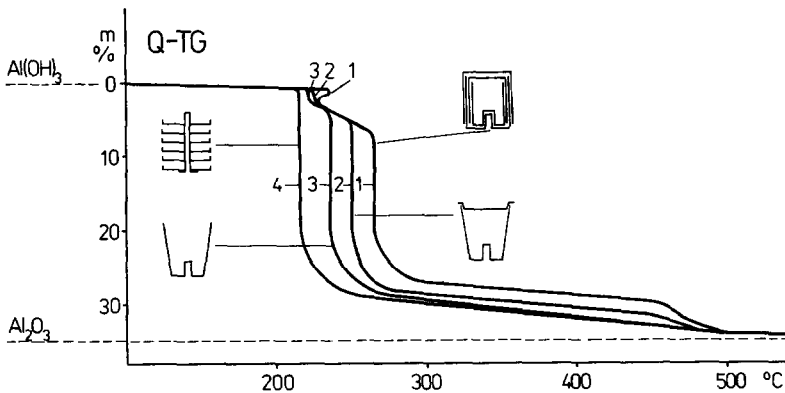
Fig. 3. Q-TG curves of artificial hydrargillite (VI) examined in a labyrinth sample holder (1), in a covered (2) and uncovered crucible (3), and on a multiplate sample holder (4).

were examined under the above mentioned experimental conditions. Four different types of sample holder were used (curves 1–4 in Figs 3–5). By changing the sample holders the aim was to change the partial pressure of the water vapour in the vicinity of the sample in order to influence the equilibrium and, along with this, the course of one of the processes with respect to the other. From the changed shape of the curve we expected to receive further useful information regarding the mechanism of the decomposition. According to experience [39], in the case of the quasi-isothermal measuring technique, by changing the sample holder the concentration of the gaseous decomposition products in the vicinity of the sample can also be significantly changed (labyrinth, 100 kPa; covered crucible, 20 kPa; uncovered crucible, 5 kPa, multiplate sample holder, 1 kPa), while the partial pressure of the gaseous product remains practically constant (quasi-isobaric) during the whole process.

In the Q-TG curves in Fig. 3 the section at about 200°C, indicating the

Fig. 4. Q-TG curves of natural hydrargillite (III) examined in a labyrinth crucible (1) in a covered (2) and uncovered crucible (3), and on a multiplate sample holder (4).
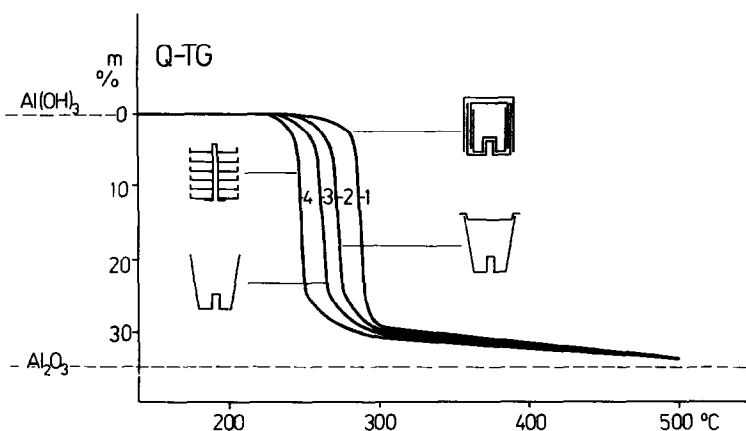
Fig. 5. Q-TG curves of natural hydrargillite (I) examined in labyrinth crucible (1), in a covered (2) and uncovered crucible (3), and on a multiplate sample holder (4).

beginning of the decomposition, shows that the sample became transitionally overheated, whereupon its temperature spontaneously dropped. We wished to study this process more thoroughly and therefore the recording of this section of the Q-TG curves was repeated by applying various decomposition rates (conversion into 100 mg total theoretical weight loss of the decomposition rates: 0.05; 0.1; 0.5; 1.0; 2.0; 5.0; 10.0 mg min^{-1} while the heating rate was 3°C in the weight-constant sections). Curves 9–15 of Fig. 6 were obtained.

We also investigated in what way the decomposition of hydrargillite would continue if for certain periods the quasi-isothermal measurement was interrupted (0.5 mg min^{-1} decomposition rate) and the sample settled in the
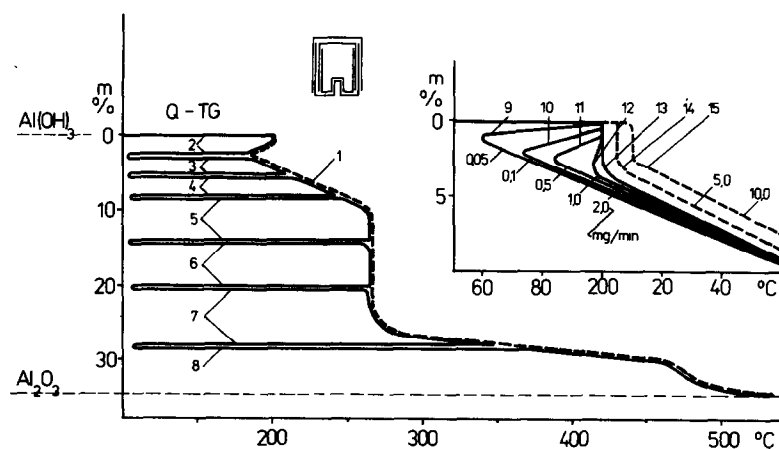
Fig. 6. Q-TG curves of artificial hydrargillite (VI) taken in the conventional way (1) on the one hand, and on the other by interrupting the examination in various stages of the transformation and recommencing it after cooling (2–8).

8

labyrinth suddenly cooled down, and thereafter the experiment recommenced [39]. The results of these examinations are illustrated by curves 2–8 in Fig. 6. Curve 1 shows the decomposition process of the sample without interruption.

The great resolution and selectivity of the quasi-isothermal–quasi-isobaric technique was also suitable for preparative purposes, viz., by producing intermediary decomposition products. Q-TG curves of samples I and VI, representing the two borderline cases, and sample III, the transitional type, were recorded using the labyrinth and multiplate sample holders and keeping the 0.3 mg min^{-1} decomposition rate (calculated for 100 mg total theoretical weight loss). However, at a given point in the decomposition the measurement was interrupted and the sample was suddenly cooled down. In this way we were able to quench the reaction and obtain the sample in its required state. Thereafter, these intermediary products were examined using X-ray examinations (Figs. 7 and 8). The applied X-ray diffraction equipment
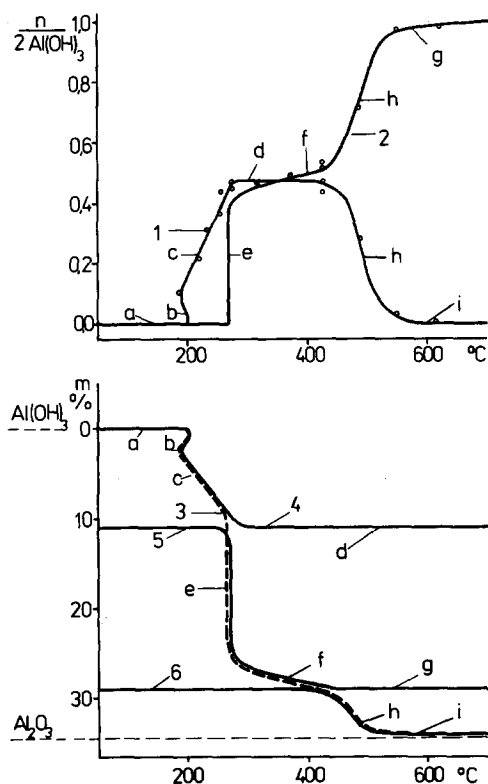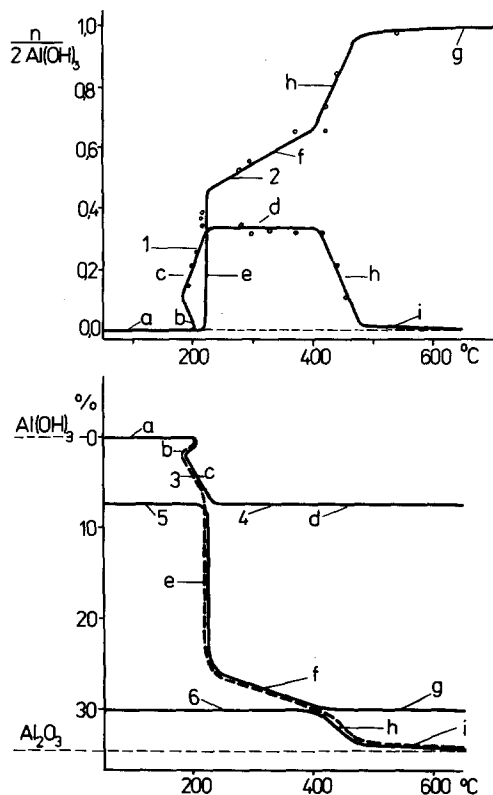

Fig. 7. Curves obtained in quasi-isothermal and X-ray measurements. (1) Changes in the amount of the boehmite formed; (2) changes in the amount of calculated Al_2O_3; (3) Q-TG curve; (4) course of the partial reaction α-Al(OH)$_3$ → α-AlOOH; (5) course of the partial reaction α-Al(OH)$_3$ → χ-Al$_2$O$_3$; (6) course of the partial reaction: α-AlOOH → γ-Al$_2$O$_3$. Sample, artificial hydrargillite (VI); sample holder, labyrinth.

Fig. 8. Curves obtained in quasi-isothermal and X-ray measurements. (1) Changes in the amount of boehmite formed; (2) changes in the amount of calculated Al_2O_3; (3) Q-TG curve; (4) course of the partial reation $\alpha\text{-Al(OH)}_3 \rightarrow \alpha\text{-AlOOH}$; (5) course of the partial reaction $\alpha\text{-Al(OH)}_3 \rightarrow \chi\text{-Al}_2O_3$; (6) course of the partial reaction $\alpha\text{-AlOOH} \rightarrow \gamma\text{-Al}_2O_3$. Sample, artificial hydrargillite (VI); sample holder, multiplate.

was a constant potential generator TuR M 62, manufactured by Transformatoren und Röntgenswerke, Dresden, in connection with a vertical goniometer PW 1050/70 and a graphite monochromator produced by Philips.

There are two possible ways of following the changes in the crystal structure: one method is based on the measurement of the intensity proportions of the selected reflexions of hydrargillite and boehmite, while the other is based on the quantitative determination of boehmite by using an inner standard. The latter method was chosen in the present work since it is more accurate.

The samples pretreated by quasi-isothermal thermogravimetry were mixed with 20% $\alpha\text{-Al}_2O_3$ and made homogeneous in ether. The integral intensities of the coincidenceless reflexions of boehmite ($d = 6.12$ Å) and $\alpha\text{-Al}_2O_3$ ($d = 2.55$ Å) in this mixture were determined by X-ray measurements.

For calibration purposes, we applied the straight

$$y = 0.109 + 0.090x \text{ (corr.: 0.993)}$$

where y is the intensity proportion ($y = I_{\text{boehmite}}/I_{\alpha\text{-Al}_2\text{O}_3}$) and x is the concentration of boehmite. According to experience this equation can be used with certainty for up to 60% boehmite content, i.e., to the concentration domain in question.

Figures 7 and 8 show the partial processes of the three-stage decomposition of hydrargillites for the case when the reaction took place under quasi-isothermal and quasi-isobaric conditions by using the labyrinth (Fig. 7) and the multiplate (Fig. 8) sample holders. The curves were constructed by calculations based on the values obtained from the Q-TG curve on the one hand, and the values of the boehmite determination by X-ray, on the other. Curve 1 shows the changes in the molecule number of boehmite calculated for 2 moles of hydrargillite, while curve 2 shows similar changes occurring in aluminium oxide. Curves 3 in Figs. 7 and 8 are Q-TG curves, and are identical in succession with curves 1 and 4 in Fig. 3. These curves represent the series of points at which the reaction was quenched to obtain intermediary products for X-ray examination. Curves 4, 5 and 6 calculated from curves 1 and 2 in Figs. 7 and 8 show the course of partial reactions corresponding to eqns. (5), (6) and (7), respectively. These curves are expressed in percentages of the weight changes. We also examined the quantity of transitionally formed boehmite in the case of samples I and VI.

DISCUSSION

What kind of partial reactions and processes make up the mechanism of the decomposition of hydrargillite? In what way and why do these differ from one another in the case of hydrargillites of various origin? What are the kinetics of these partial processes and how are they influenced by the experimental conditions? The answers to these questions proved to be complex, as is the reaction mechanism itself, the subject of this problem. For the last mentioned, the following mosaic-like picture can be brought together if we arrange the mass of data obtained from Figs. 1–8.

In general, it can be stated that the decomposition of hydrargillites is composed of three overlapping partial reactions (curves 4, 5 and 6 in Figs. 7 and 8). These reactions can be discribed by eqns. (5), (6) and (7)

$$\alpha\text{-Al(OH)}_3 \rightarrow \alpha\text{-AlOOH} + H_2O \tag{5}$$

$$2\ \alpha\text{-Al(OH)}_3 \rightleftharpoons \chi\text{-Al}_2\text{O}_3 + 3\ H_2O \tag{6}$$

$$2\ \alpha\text{-AlOOH} \rightleftharpoons \gamma\text{-Al}_2\text{O}_3 + H_2O \tag{7}$$

Each of these decomposition reactions is divided into several parts (curve sections a–i in Figs. 7 and 8).

Conversion of hydrargillite into boehmite

If the decomposition is composed of three stages, then first boehmite would be formed (curves 1 and 4 in Figs. 7 and 8). This process is generally introduced by nucleus formation which is indicated in the Q-TG curves by a transitional overheating of the sample (section b curves 1 and 4 in Figs. 7 and 8). This occurs because, due to the delayed start of nucleus formation, the heating control system transitionally raises the temperature of the sample over the transition temperature. The nucleus formation can begin only at a higher energy level of the sample. After nucleus formation has started the temperature of the sample spontaneously drops because along with the increase in the number of nuclei, a gradually lower and lower temperature is necessary so that the weight loss takes place at the prescribed rate [39].

With this it can also be explained that the course of this section of the Q-TG curves depends on the decomposition rate we have programmed (curves 9–15 Fig. 6). In the case of a low rate (curve 9, Fig. 6) the sample cools down to a greater extent than in the case of higher decomposition rates (curve 12).

It is noteworthy that the temperature at the start of nucleus formation, up to the given 200°C limit, is independent of the decomposition rate (curves 9–13, Fig. 6). If a higher rate of decomposition than is necessary is chosen, the temperature of the sample cannot fall any more (curve 13, Fig. 6). What is more, it can happen that the start of decomposition will be shifted above the characteristic temperature of 200°C (curves 14 and 15, Fig. 6). The thermal decomposition of such types of hydrargillites also starts at 200°C if a dynamic heating program is applied (curves 4, 5 and 6 in Figs. 1 and 2).

The reaction of boehmite formation is not a process which leads to equilibrium since by changing the sample holders, i.e., by changing the concentration of the gaseous decomposition products in the vicinity of the sample, the course of the transformation (curves 1–4, Fig. 3) cannot be influenced at all [39].

However, by changing the sample holders the amount of the boehmite formed can be varied (curves 1 and 4, Figs. 7 and 8). The larger the partial pressure of the water vapour formed in the vicinity of the sample the larger the amount of boehmite. The explanation of this phenomenon is probably two fold; on the one hand, the reactions

$$\alpha\text{-Al(OH)}_3 \rightarrow \alpha\text{-AlOOH}$$

and
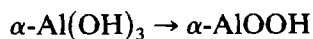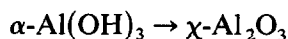
$$\alpha\text{-Al(OH)}_3 \rightarrow \chi\text{-Al}_2\text{O}_3$$

are competitive and when the latter begins, the former is nearly completed (section d in curves 1 and 4, Figs. 7 and 8), and on the other, the beginning of the reaction α-Al(OH)$_3$ $\rightarrow$ χ-Al$_2$O$_3$ was delayed (curves 1 and 4 in Fig. 3)

by using the labyrinth crucible instead of the multiplate sample holder, and so the initial temperature of this process increased from 220°C to 265°C. Accordingly, in the latter case more boehmite could be formed, since it took longer for the temperature to rise from 200 to 265°C, instead of 220°C.

It can also be stated that the progress of the boehmite formation continuously and proportionately increases the temperature of transformation (section c of curves 1 and 4, Figs. 7 and 8). Every single value of the latter curve is characteristic to the actual state of the materials [39]. According to the course of curves 2, 3 and 4 in Fig. 6, viz. when we recommenced the experiment after quenching, the process continued at the very same temperature at which the experiment was interrupted.

*Conversion of hydrargillite to χ-aluminium oxide*

This reaction [eqn. 6] consists of two partial processes (sections e and f of curves 2 and 5, Figs. 7 and 8). According to the Q-TG curves (curves 1–4, Fig. 3) the first process leads to equilibrium while the second one does not. Therefore, by changing the labyrinth crucible for the multiplate sample holder, the first process would take place at 220°C instead of 265°C, while the temperature of the second process cannot be influenced in a similar way.

The two processes also differ from one another in that the first one takes place in a quasi-isothermal way and if the rate of the heat absorption of the sample and the partial pressure of the water vapour in the vicinity of the sample do not change, then both the rate of the decomposition and temperature of the transformation stay constant (curves 1–4, Fig. 3). In contrast, the second process of the transformation (section f of curves 2 and 5, Figs. 7 and 8) can proceed with the prescribed rate only if the temperature is continuously and significantly increased. As in the case of the transformation

$$\alpha\text{-Al(OH)}_3 \rightarrow \alpha\text{-AlOOH}$$
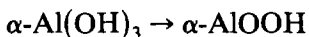
for every temperature and every state of the transformation process, there corresponds a defined state of the material [39], i.e., a defined water content and inner structure (Fig. 6). This becomes understandable if we accept the supposition of Freund [40] according to which in general the water release from hydroxyl groups is the result of the movement of protons. The probability of this process decreases with the reduction of the number of OH-groups and therefore the release of the remaining OH-group requires a greater energy, i.e., a higher temperature.

From the Q-TG curves it can also be read that the two reactions

$$\alpha\text{-Al(OH)}_3 \rightarrow \alpha\text{AlOOH}$$

and
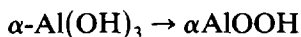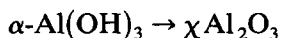
$$\alpha\text{-Al(OH)}_3 \rightarrow \chi\text{Al}_2\text{O}_3$$

are really competitive and do not overlap. In the reverse case, it would be

expressed in the course of the Q-TG curves [39]. If the isothermal transformation α-Al(OH)$_3$ $\rightarrow$ αAlOOH and the non-isothermal conversion α-Al(OH)$_3$ $\rightarrow$ χ-Al$_2$O$_3$ had taken place simultaneously, the corresponding section of the Q-TG curves (section e of curves 2 and 5, Fig. 7) would not be of isothermal character, but would have extended to a more or less broad temperature interval.

Conversion of boehmite to γ-aluminium oxide

In the vicinity of 400°C only χ-Al$_2$O$_3$ and α-AlOOH remain (curves 1 and 2, Figs. 7 and 8). Above this temperature the decomposition of boehmite also begins [eqn. (7)], and according to the Q-TG curves in Fig. 3 this reaction is practically complete by 500°C. The weight loss observed in the mentioned temperature interval is proportional to the amount of boehmite formed (section h of curves 1 and 6, Figs. 7 and 8). The proportionality between the first and third peaks of the DTG curves [33–37] can also be attributed to this circumstance (Figs. 1 and 2). This reaction also leads to equilibrium (enlarged curves 1–4, Fig. 3). The residue gradually looses the remaining water (section i of curves 1 and 6, Figs. 7 and 8) which is in accordance with the theory of Freund [40].

By comparing the two borderline cases, represented by the three-stage decomposition of artificial hydrargillites (Figs. 3, 7 and 8) on the one hand, and the one-stage decomposition of hydrargillites of natural origin (Fig. 5) on the other, it can be stated that the only difference between them is that in the former a significant amount of intermediary boehmite is being formed (curve 1, Figs. 7 and 8) while in the latter the amount of boehmite formed is insignificant.

Those natural and artificial hydrargillites whose thermoanalytical curves form a transition between the two borderline cases (Fig. 4) differ from one another—at least from the point of view of their decomposition—only with respect to the amount of boehmite formed.

Further observations and conclusions regarding the decompostion mechanism of hydrargillites will be reported in the second part of this work.

REFERENCES

1 K. Wefers and G.M. Bell, ALCOA (Alum. Co. Am.) Res. Lab., Tech. Pap. No. 19 (1972) 8, 36.

2 F. Haber, Naturwissenschaften, 13 (1925) 1007.

3 F.C. Frary, Ind. Eng. Chem., 38 (1946) 129.

4 Z.D. Zivkovic, Thermochim. Acta, 21 (1977) 391.

5 H.C. Stumpf, A.S. Russel, J.W. Newsome and J.W. Tucker, Ind. Eng. Chem., 42 (1950) 1398.

6 R. Tertian, Bull. Soc. Chim. Fr., 18 (1951) 384.

7 M.K.B. Day and V.J. Hill, Nature (London), 170 (1952) 539.

8 M.K.B. Day and V.J. Hill, J. Phys. Chem., 57 (1953) 946.

9 K. Sasvári and A.J. Hegedüs, Naturwissenschaften, 42 (1955) 254.

10 K. Sasvári, Acta Geol. Acad. Sci. Hung., 4 (1957) 415.

11 J. Beretka and M.J. Ridge, J. Chem. Soc. London, Ser. A, (1967) 2106.

12 K.N. Goswami and A.K. Grupta, Trans. Indian Ceram. Soc., 36 (1) (1977) 7.

13 H. Ginsberg, W. Hüttig and G. Strunck-Lichtenberg, Z. Anorg. Allg. Chem., 293 (1958) 33, 204.

14 T. Sato, F. Ozawa and S. Ikoma, Thermal Analysis, ICTA 80, Birkhauser Verlag, Basel, Boston, Stuttgart, p. 181.

15 J.F. Brown, D. Clark and W.W. Elliot, J. Chem. Soc., (1953) 84.

16 J.H. De Boer, J.M.H. Fortuin and J.J. Steggerda, Proc. K. Ned. Akad. Wet. B, 57 (1954) 170, 434.

17 R. Tertian, D. Papeé and J. Charrier, C.R., 238 (1954) 98.

18 S. Saalfeld, Neues Jahrb. Mineral., Abh., 95 (1) (1960) 1.

19 A.M. Kalinina, Zh. Neorg. Khim., 4 (6) (1959) 1260.

20 O. Glemser and G. Rieck, Z. Angew. Chem., 67 (1955) 652.

21 J. Rouquerol, F. Rouquerol and M. Ganteaume, J. Catal., 36 (1975) 99.

22 J. Rouquerol, F. Rouquerol and M. Ganteaume, J. Catal., 57 (1979) 22.

23 J.A. Lewis and C.A. Toyler, J. Appl. Chem., 8 (1958) 223.

24 R. Tertian and D. Papeé, J. Chem. Phys., 55 (1958) 341.

25 T. Sato, J. Appl. Chem., 6 (1959) 207.

26 K.R. Funaki and Y.K. Shimiza, Kogya Kagaku Zasshi, 62 (1959) 782.

27 R.C. Mackenzie, Differential Thermal Analysis, Academic Press, London, New York, 1970, p. 283.

28 W. Lodding, Proc. Int. Conf. Therm. Anal., 1968, Vol. 2, Academic Press, New York, 1969, p. 1239.

29 K. Wefers, Erzmetall, XVII (1964) 583.

30 D. Papeé and R. Tertian, Bull. Soc. Chim. Fr., 22 (1955) 983.

31 T.A. Arlyunk and T.V. Telyatnikov, Tsvetn. Metall., (1977) (8) 44.

32 P.C. Sen, Ashimesh Dutt and H.V. Bhaskar Rao, Trans. Indian Ceram. Soc., 32 (3) (1973) 60.

33 L. Erdey and F. Paulik, Acta Chim. Acad. Sci. Hung., 7 (1955) 45.

34 F. Paulik and L. Erdey, Acta Chim. Acad. Sci. Hung., 13 (1957) 117.

35 L. Erdey and F. Paulik, Acta Chim. Acad. Sci. Hung., 21 (1959) 205.

36 F. Paulik, J. Paulik and L. Erdey, Anal. Chim. Acta, 41 (1968) 170.

37 F. Paulik and J. Paulik, Thermochim. Acta, 4 (1972) 189.

38 F. Paulik and J. Paulik, J. Therm. Anal., 5 (1973) 253.

39 J. Paulik and F. Paulik, in G. Svehla (Ed.), Comprehensive Analytical Chemistry, Vol. XII, Part A, Elsevier, Amsterdam, 1981.

40 F. Freund, Fortschr. Chem. Forsch., 10 (1968) 347.